

## Critical behavior at dynamical phase transition in the generalized Bose-Anderson model

Dmitry V. Chichinadze\* and Alexey N. Rubtsov

*Russian Quantum Center, Novaya 100, 143025 Skolkovo, Moscow Region, Russia*  
*and Department of Physics, Lomonosov Moscow State University, Leninskie gory 1, 119991 Moscow, Russia*

(Received 24 January 2017; revised manuscript received 28 April 2017; published 18 May 2017)

Critical properties of the dynamical phase transition in the quenched generalized Bose-Anderson impurity model are studied in the mean-field limit of an infinite number of channels. The transition separates the evolution toward ground state and toward the branch of stable excited states. We perform numerically exact simulations of a close vicinity of the critical quench amplitude. The relaxation constant describing the asymptotic evolution toward ground state, as well as asymptotic frequency of persistent phase rotation and number of cloud particles at stable excited state are power functions of the detuning from the critical quench amplitude. The critical evolution (separatrix between the two regimes) shows a non-Lyapunov power-law instability arising after a certain critical time. The observed critical behavior is attributed to the irreversibility of the dynamics of particles leaving the cloud and to memory effects related to the low-energy behavior of the lattice density of states.

DOI: [10.1103/PhysRevB.95.180302](https://doi.org/10.1103/PhysRevB.95.180302)

The dynamics of correlated quantum systems that show phase transitions at their equilibrium became a subject of intensive investigations in the last decade. One of the key differences between the classical and quantum ensembles is that the latter can exhibit the undamped (persistent) excitations such as, for example, vortices in the superfluids and superconductors [1–3]. Therefore, whereas a generic nonlinear classical system at finite temperature is ergodic, a quantum fluid is not necessarily. This gives rise to phase transitions seen in the asymptotic dynamics of an open quantum system: dependent on initial conditions, it can either relax to its ground state or not. The two regimes are separated by the dynamical transition point. In a wider context, dynamical transitions are singularities arising in the many-body quantum dynamics. In particular, several models show a critical time  $t^*$  after which an instability develops [4–6].

The studies of how the criticality shows up in the dynamics have a long history but firstly have been mostly devoted to classical systems. It was found that the dynamical critical exponents arise (see [7,8]). The most known is the  $Z$  index relating the correlation length  $\xi$  and the relaxation time  $\tau$  via  $\tau \propto \xi^Z$  [7,9]. The values of dynamical indexes cannot be expressed via static ones (that is, a dynamical effective Hamiltonian obeys a larger number of relevant parameters than its static counterpart). Moreover, varying parameters of a system within the same static universality class, one can obtain different values of dynamical indexes. To describe such a situation the dynamical subclasses have been introduced [10].

The dynamical quantum criticality was reported in a number of recent works [4,5,11] where the dynamics of the transverse-field Ising model in low dimensions has been studied. Loschmidt echo rate scaling [5] was described using the renormalization group performed in a complex parameter space. However, the universality of this procedure has been questioned in a very recent work [12]. Unfortunately the results of this work are also very model specific as the

after-quench Hamiltonian is purely classical. Generic evidence about the criticality emerged in quantum dynamics remains very limited because of numerical issues. The quantum Monte Carlo (QMC) method is almost the only numerically exact approach to simulate a generic system on a lattice. However the long-time QMC calculations of high accuracy are complicated because of the growing sign problem. Nevertheless dynamical transitions have been observed in QMC calculations of Hubbard-like models [13,14], although the dynamical scaling was not studied.

Phase transitions are usually associated with translationally invariant systems, but in the quantum case they can also emerge in so-called impurity problems, that is, in localized (zero-dimensional) nonlinear systems coupled to a Gaussian thermostat. In particular, this is the case for the Bose-Anderson model [15], which describes a 2-4 nonlinear oscillator connected to the Gaussian lattice obeying a power-law density of states. This model is closely related to the celebrated Dicke model [16,17]. Although the nonlinearity is localized at a single spatial point, a spontaneous symmetry breaking of the ground state can occur [18,19]. The phase diagram contains high- and low-symmetry phases, respectively called local Mott insulator (IMI) and local Bose-Einstein condensate (IBEC).

In our recent paper [20], we have shown that impurity models can exhibit dynamical phase transitions as well. We have studied the generalized Bose-Anderson model, in which  $N$  identical nonlinear oscillators are connected to the same lattice site. For  $N \rightarrow \infty$  the mean-field treatment of the model becomes exact, allowing for a simple numerical handling of its real-time dynamics. It was found that the symmetry-broken state of the system, being subjected to a quench of parameters, either relaxes to the new ground state or reaches a stable excited state, dependent on the quench amplitude. The two asymptotic regimes are separated by a dynamical transition.

In the present Rapid Communication, we perform a systematic study of the quenched generalized Bose-Anderson model and conclude that the dynamical phase transition is a generic property of the IBEC phase. Further, we investigate a vicinity of the dynamical transition. We detect the power-law dependence of the asymptotic evolution characteristics from

\*Present address: School of Physics and Astronomy, University of Minnesota, Minneapolis, MN 55455, USA; [chich013@umn.edu](mailto:chich013@umn.edu)

the detuning of the quench amplitude from its critical value. Moreover, after a critical time  $t^*$  the evolution itself appears to be unstable with a power-law type of instability. Our numerics suggests that the observed critical indexes are simple fractions, as one would expect for an  $N \rightarrow \infty$  case.

The Hamiltonian of the generalized Bose-Anderson model reads [20]

$$\hat{H} = \sum_j H_{\text{SI}}[\hat{a}_j^\dagger \hat{a}_j] - \sum_{j,k} \frac{V}{\sqrt{N}} (\hat{a}_j^\dagger \hat{b}_k + \hat{b}_k^\dagger \hat{a}_j) + \sum_k \epsilon_k \hat{b}_k^\dagger \hat{b}_k, \quad (1)$$

where

$$\hat{H}_{\text{SI}}[\hat{a}_j^\dagger \hat{a}_j] = \epsilon_0 \hat{a}_j^\dagger \hat{a}_j + \frac{1}{2} \hat{a}_j^\dagger \hat{a}_j^\dagger \hat{a}_j \hat{a}_j \quad (2)$$

is the Hamiltonian of a single component of the impurity,  $\hat{a}^\dagger, \hat{a}$  and  $\hat{b}^\dagger, \hat{b}$  are creation-annihilation operators acting as impurities numbered with  $j$  and lattice modes numbered with  $k$ , respectively,  $\epsilon_0$  is the impurity on-site potential, and  $V$  determines the coupling between impurities and the lattice. Following our previous paper we consider a cubic lattice, so that  $\epsilon_k = 2h[3 - \cos(k_x) - \cos(k_y) - \cos(k_z)]$ , and assume  $h = 1$ . The  $\mathbf{k} = 0$  mode is excluded from the Hamiltonian to remove the effects related to Bose-Einstein condensation in the bulk of the lattice.

In the limit of  $N \rightarrow \infty$ , the effect of the lattice is reduced to a classical field  $\lambda$  acting on the impurity, so that the system is described by the effective Hamiltonian

$$H^{\text{eff}} = \epsilon_0 \hat{a}^\dagger \hat{a} + \frac{1}{2} \hat{a}^\dagger \hat{a}^\dagger \hat{a} \hat{a} - \lambda \hat{a}^\dagger - \lambda^* \hat{a}. \quad (3)$$

In the symmetry-broken IBEC phase the self-consistency condition

$$\lambda_{\text{eq}} = \sum_k \frac{V^2}{\epsilon_k} \langle a \rangle \quad (4)$$

holds with a nonzero order parameter  $\langle a \rangle$ ; the average is taken over the ground state of (3) with  $\lambda_{\text{eq}}$  substituted. For the IMI phase this equation is trivially fulfilled with  $\langle a \rangle = 0$ ,  $\lambda_{\text{eq}} = 0$ . The equilibrium phase diagram of the model is shown in the lower panel of Fig. 1. We study a type of quenches for which a dynamical transition was reported in [20]. They correspond to a sudden lowering  $-\epsilon_0$  within the IBEC domain for the system initially prepared in its ground state.

Out of equilibrium the field  $\lambda$  is time dependent and has a memory about the past:

$$\lambda(t) = \sum_k V^2 \frac{e^{-i\epsilon_k t}}{\epsilon_k} \langle a(0) \rangle + i \sum_k V^2 \int_0^t \langle a(t') \rangle e^{-i\epsilon_k(t-t')} dt'. \quad (5)$$

Possible asymptotic states of the system described by (5) are either the new equilibrium state, or the stable excited state with a persistently rotating phase  $\langle a(t) \rangle = a_\infty e^{i\omega t}$ . The value of  $a_\infty$  can be found by switching to the rotation frame [20], where the chemical potential appears to be shifted;  $\epsilon_0 \rightarrow \epsilon_0 + \omega$ ,  $\epsilon_k \rightarrow \epsilon_k + \omega$ . After this shift is accounted for,  $a_\infty$  satisfies the ‘‘equilibrium’’ equations (3) and (4). As is immediately seen,  $\omega$  must be positive: the chemical potential shift causes instability otherwise. An appearance of the stable excited states is related to the relaxation mechanism of the model: the excited system loses its energy by the emission of bosons away from the

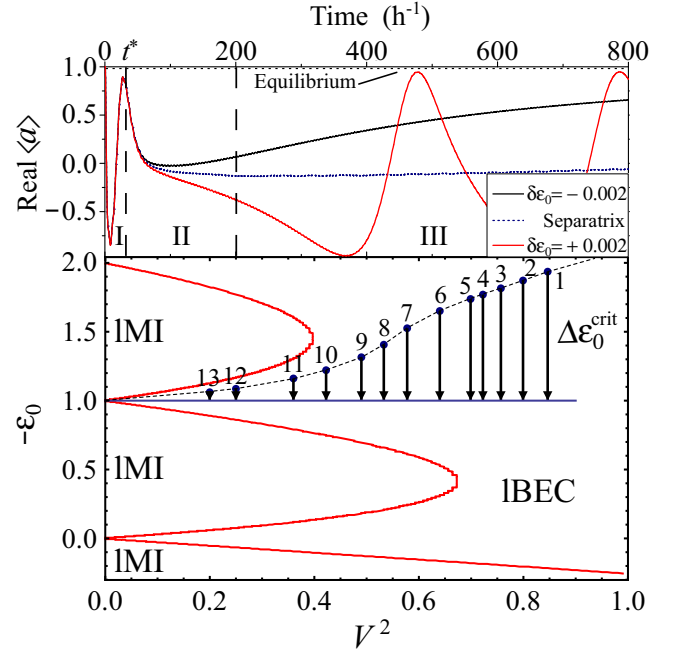


FIG. 1. Upper panel: time evolution of the real part of the order parameter for three different quench amplitudes. The dotted line depicts the time evolution for the critical quench amplitude (separatrix); the black and red lines correspond to quenches with detuning  $\delta\epsilon_0 = \pm 0.002$  from the critical value. The black line corresponds to a solution relaxing to the new equilibrium state, while the red line corresponds to a stable excited state (rotating phase). Lower panel: critical quenches plotted on an equilibrium phase diagram of the model. The dashed line and dots depict positions on the phase diagram from which the critical quench takes place.

impurity and the surrounding cloud [20]. Stable excited states have less particles than the equilibrium state and therefore cannot relax. In particular, an increase of  $-\epsilon_0$  always results in an excited state, as the new ground state requires a larger amount of particles than exists in the system.

Lowering  $-\epsilon_0$ , one observes the quenched dynamics toward one of the two different asymptotic regimes. For a small positive quench amplitude  $\Delta\epsilon_0 = \epsilon_0(t > 0) - \epsilon_0(t < 0)$ , loss of particles results in an evolution toward the new ground state. Increasing  $\Delta\epsilon_0$ , with no change in  $\epsilon_0(t > 0)$ , results in the formation of the persistently rotating phase. The two scenarios are separated by the dynamical transition singularity occurring at certain  $\Delta\epsilon_0^{\text{crit}}$ .

The lower panel of Fig. 1 shows critical quenches plotted on the equilibrium phase diagram. We have performed simulations for a number of final quench points ( $V, -\epsilon_0$ ) along the line  $-\epsilon_0 = 1$  separating two local Mott lobes. The described dynamical transition was observed for all points including those lying between the lobes: smaller  $V$  corresponds to narrower IBEC strip, and also to smaller critical quench value. Inside the IBEC phase, the transition does not show a link to the equilibrium phase diagram and is therefore interpreted as a purely dynamical phenomenon. This makes quenches within IBEC different from those involving the IMI phase [20], whose transient dynamics is closely related with the equilibrium phases on the quench path.

In our study we examined a close vicinity of the critical quenches. Let us introduce the deviation of the quench amplitude from the critical value  $\delta\varepsilon_0 = \Delta\varepsilon_0^{\text{crit}} - \Delta\varepsilon_0$ ; negative (positive)  $\delta\varepsilon_0$  corresponds to the quenches below (above) the critical value. In our calculations, values of critical quench amplitudes were estimated with an accuracy of at least  $10^{-3}$ . The upper panel of Fig. 1 shows the time dependence of the order parameter for three quench amplitudes: right at the dynamical transition ( $\delta\varepsilon_0 = 0$ —this curve can be called separatrix), slightly above and slightly below the critical quench value. A closer look at the numerical data shows that the three characteristic time intervals can be introduced. Within the interval I, up to critical time  $t^*$  (indicated by the vertical dashed line in Fig. 1, upper panel) the deviation  $\delta a(t) = \langle a(t) \rangle - \langle a_{\text{crit}}(t) \rangle$  does not significantly change. For  $t > t^*$ , the evolution becomes unstable:  $\delta a(t)$  increases with time. We introduce time interval II, where  $\delta a$  grows in time, but still remains small compared to  $\langle a \rangle$ . The asymptotic evolution is realized in the interval III, where  $\delta a$  and  $\langle a \rangle$  are of the same order. Note that whereas  $t^*$  is independent of  $\delta\varepsilon_0$ , the crossover between the time intervals II and III occurs at larger time arguments for smaller  $\delta\varepsilon_0$ .

We address the following questions: (i) concerning the time interval III, how the equilibration occurs for small negative  $\delta\varepsilon_0$  and how asymptotic rotation frequency behaves for small positive  $\delta\varepsilon_0$ ; and (ii) concerning the time interval II, what is the type of instability for the separatrix.

An analysis of the equilibration at  $\delta\varepsilon_0 < 0$  has shown that the asymptotic deviation of the order parameter from its equilibrium value falls exponentially with time. The upper panel of Fig. 2 provides an example of the exponential fit  $\langle a \rangle(t) = a_{\text{eq}} - a_1 e^{-\sigma t}$  at  $\delta\varepsilon_0 = -0.0219$  for the quench to ( $V = 0.894$ ,  $-\varepsilon_0 = 1$ )—the quench 2 from Fig. 1. Values of the relaxation constant  $\sigma$  obtained from the fitting procedure show a square-root dependence on  $|\delta\varepsilon_0|$ , as the lower panel of Fig. 2 shows: we plot  $\sigma^2$  vs  $\delta\varepsilon_0$  and observe a linear dependence. The same panel presents our results for the asymptotic rotation frequency for the system being quenched with  $\delta\varepsilon_0 > 0$  to the same point ( $V = 0.894$ ,  $-\varepsilon_0 = 1$ ). In this case  $\omega^3$  (the right axis) exhibits linear dependence, so that we conclude about  $\omega \propto (\delta\varepsilon_0)^{1/3}$ .

Our conclusions allow one to estimate how the number of particles asymptotically remaining in the IBEC cloud  $N_{\text{IBEC}}$  scales with  $\delta\varepsilon_0$ . The rotation-frame analysis [20] gives the expression  $N_{\text{IBEC}} \propto \int \frac{d^3k}{(\omega + \epsilon_k)^2}$ . It leads to the divergence  $N_{\text{IBEC}} \propto \omega^{-1/2}$ . We consequently conclude about the scaling law  $N_{\text{IBEC}} \propto (\delta\varepsilon_0)^{-1/6}$  at small positive  $\delta\varepsilon_0$ .

Now let us turn to the analysis of the instability of the critical evolution at  $t > t^*$ , i.e., in the interval II. Figure 3 presents a log-log plot of  $|\delta a(t - t^*)|$  calculated for a set of quenches with different impurity-lattice coupling  $V$ ; the values of  $t^*$  vs  $V$  are plotted in the inset. For each quench, we have considered two values of  $\delta\varepsilon_0 = \pm 5 \times 10^{-4}$ . It appears that the sign of  $\delta\varepsilon_0$  almost does not affect the absolute value of  $|\delta a|$ . For each quench, Fig. 3 shows two dependencies of  $|\delta a(t - t^*)|$ , which correspond to the positive and negative  $\delta\varepsilon_0$ , but these two dependencies are almost indistinguishable from each other. Besides small high-frequency oscillations, possibly related to the upper cut-off introduced by a discrete lattice, the log-log

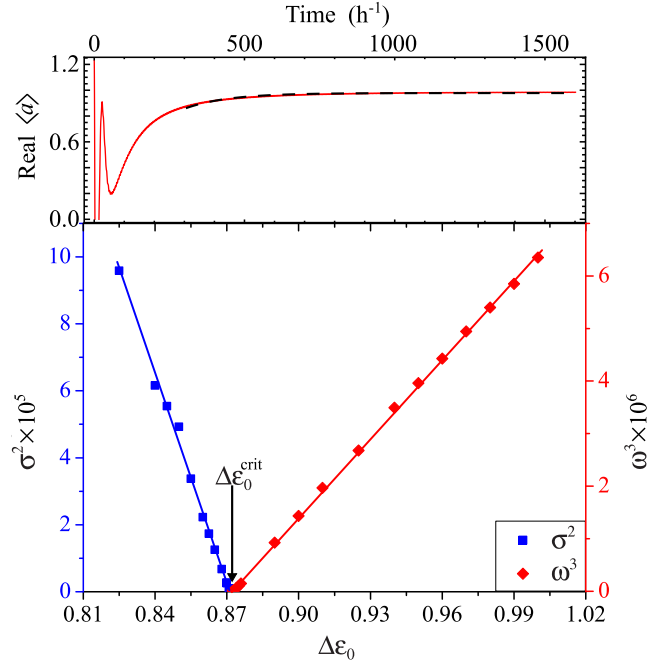


FIG. 2. Upper panel: exponential fit of equilibration asymptotic dynamics. Red curve shows the dynamics of the real part of the order parameter, while the black dashed one depicts exponential fit. Lower panel: power-law dependencies of relaxation parameter  $\sigma$  (blue dots) and frequency  $\omega$  (red dots) as functions of quench amplitude  $\Delta\varepsilon_0$ . In this picture the critical quench amplitude is  $\Delta\varepsilon_0^{\text{crit}} = 0.8719$ . As seen from the picture,  $\sigma \propto (\delta\varepsilon_0)^{1/2}$  and  $\omega \propto (\delta\varepsilon_0)^{1/3}$ .

curves shown in Fig. 3 remain linear while the time argument is changed by two orders of magnitude; however, this range is narrowed for the quench 9 performed for the smallest  $V$ , i.e., closer to the IMI region.

We conclude about the power-law dynamical instability  $\ln|\delta a| \propto \ln(t - t^*)$  with the index being the same for all quenches. We remind one that the usual scenario known from the nonlinear dynamics of classical finite systems is the Lyapunov instability [21]: a small deviation from the separatrix trajectory grows in time exponentially. For the system considered, this does not appear to be the case.

The exact index value extracted from the numerical data slightly depends on how the values of  $t^*$  are chosen. A finite value of  $\delta\varepsilon_0$  used in calculations corresponds to a finite region where a stable evolution passes into the power-law instability; this results in certain error bar for the value  $t^*$ . We have performed estimations of the index for  $t^*$  taken within this region and obtained the index close to 1.30 with an error bar of about 0.03. The mean value 1.30, as well as the log-log dependencies shown in Fig. 3, are obtained for  $t^*$  fitted to minimize the crossover region between the stable and power-law evolution. For comparison, we have drawn straight lines in Fig. 3 corresponding to the indexes 1.3 and  $4/3$ .

We interpret the index obtained as a critical exponent of the dynamical transition occurring at  $t^*$ . Additional comments are needed at this point, because it is not *a priori* clear if the concept of criticality is applicable for the system studied.

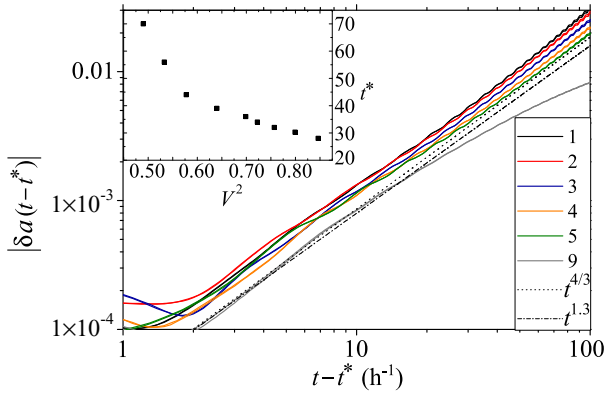


FIG. 3. The dependence of  $|\delta a(t-t^*)| = |\langle a(t-t^*) \rangle - \langle a_{\text{crit}}(t-t^*) \rangle|$  on  $t-t^*$ , where  $\langle a \rangle_{\text{crit}}$  corresponds to critical quench with  $\delta\varepsilon_0 = 0$ . One can consider this quantity as a divergence of trajectories in phase space (as is commonly considered in nonlinear dynamics), which shows the kind of instability of a critical point. Numbers of curves correspond to numbers of critical quenches shown in Fig. 1. Two lines with the same color (almost on top of each other) depict curves for quenches with  $\delta\varepsilon_0 = \pm 0.0005$ . The dashed line shows a power-law fit with power  $4/3$  and the dash-dotted line depicts a power-law fit with power  $1.3$  for these dependencies. Inset: dependence of critical time  $t^*$  on  $V$ .

Indeed, transitions at equilibrium, for which the theory of criticality was initially developed, occur in (on average) uniform systems, whereas we deal with a localized one. Another seminal example of a critical behavior is known from the Feigenbaum's [21,22] theory for the transition between the periodic and chaotic one-dimensional mapping. In this case, the localized in space system is out of equilibrium, but the very difference from our case is that the Feigenbaum's theory describes a steady process. Nevertheless our data reported above suggest that our system shows a critical behavior. The power-law instability signals that the phenomenon exhibits collective behavior: a few-body dynamics at finite time scale would be likely characterized by a Lyapunov exponent [21]. In this regard we emphasize that the memory kernel of the lattice response in Eq. (5) obeys a long memory which makes the mathematical difference of our model from a finite set of differential equations common for nonlinear dynamics. Furthermore, the very same dependence of  $|\delta a|$  on  $|\delta\varepsilon_0|$  on different sides of the transition reported in Fig. 3, excludes scenarios related to locking of some states. etc. On the other hand, it resembles the transitions at equilibrium, when fluctuations show the same behavior below and above the transition point.

Another property worth discussing is that the dynamical transition studied is not followed by a symmetry change: the order parameter does not equal zero either at the IBEC ground state, or in the state with the persistently rotating phase. The latter can be seen as a ground state of the Hamiltonian in the rotating frame, where the spectrum is gapped with the gap  $\omega$ . The situation, when the two states have the same symmetry, but one of them is gapped and another is not, is known for the equilibrium quantum phase transitions. For example, this is the

case for Mott metal-insulator transitions [23,24] (here we refer to the Mott transition which does not break the translational symmetry and leave out possible antiferromagnetism in Mott systems). As well, equilibrium quantum transitions occurring inside a symmetry-broken phase are known: an example is ferroelectric transitions in the crystals lacking inversion symmetry (e.g., in  $\text{ArCrS}_2$  [25]).

Finally, possible experimental relevance is to be discussed. In this context we consider of high importance the finding that the dynamical transition was observed in a large part of the IBEC phase, including the weak-coupling limit  $V \rightarrow 0$ . In this limit the generalized Bose-Anderson Hamiltonian is closely related to the Dicke model [3,16], as just two impurity levels are important. That is, the dynamical transition can be looked for in qubit systems where spontaneous symmetry breaking emerges (provided proper density of photon states). Another possibility is to operate with ultracold atoms. In this case, a Josephson current [26] between the IBECs of two systems with slightly different quench values can be used to measure their relative phase.

Let us present some preliminary argumentation about the applicability of our results to finite- $N$  systems, although a consideration beyond mean field is out of the scope of this Rapid Communication. We expect that the dynamical transition studied can also be found away from mean field, in the impurity systems obeying two properties: (i) the symmetry-broken phase is characterized by an infinite number of particles in the IBEC cloud surrounding the impurity and (ii) an irreversibility of dynamics of the particles leaving the cloud, which gives rise to stable excited states having less particles and higher energy than the ground state. The first property was indeed observed in the numerical renormalization group calculations for the single-impurity Bose-Anderson model [18]. The second is a simple property generic to all systems where the particles evaporate in vacuum. Quantitative properties of the transition, such as index values, can be altered from the  $N \rightarrow \infty$ . However, we mention that in some cases even index values found from mean-field grounds appear to be quite accurate; a good example is the Flory description of self-avoiding chains [27].

To summarize, using the mean-field approach we have studied the dynamical phase transition, arising within the symmetry-broken phase of the generalized Bose-Anderson impurity model. We have studied a vicinity of the transition point and found that characteristics of the asymptotic evolution (namely, the relaxation parameter and the frequency of persistent oscillations) are power functions of the detuning from the critical quench amplitude. Furthermore, the critical evolution (separatrix) also shows a non-Lyapunov power-law instability, arising after a critical time  $t^*$ . We attribute the observed phenomena to the irreversibility of the dynamics of particles leaving the IBEC cloud and to the memory effects related to the low-energy behavior of the lattice density of states.

We acknowledge useful discussions with Pedro Ribeiro, Georg Rohringer, and Yulia Shchadilova. The authors thank the Dynasty Foundation and RFBR (Grant No. 16-32-00554) for financial support.

- [1] G. L. Warner and A. J. Leggett, *Phys. Rev. B* **71**, 134514 (2005).
- [2] E. A. Yuzbashyan, O. Tsypliyatyev, and B. L. Altshuler, *Phys. Rev. Lett.* **96**, 097005 (2006).
- [3] E. A. Yuzbashyan, M. Dzero, V. Gurarie, and M. S. Foster, *Phys. Rev. A* **91**, 033628 (2015).
- [4] M. Heyl, A. Polkovnikov, and S. Kehrein, *Phys. Rev. Lett.* **110**, 135704 (2013).
- [5] M. Heyl, *Phys. Rev. Lett.* **115**, 140602 (2015).
- [6] A. Mitra, *Phys. Rev. Lett.* **109**, 260601 (2012).
- [7] G. Ódor, *Rev. Mod. Phys.* **76**, 663 (2004).
- [8] S. Sachdev, *Quantum Phase Transitions*, 2nd ed. (Cambridge University Press, Cambridge, England, 2011).
- [9] P. C. Hohenberg and B. I. Halperin, *Rev. Mod. Phys.* **49**, 435 (1977).
- [10] V. Popkov, A. Schadschneider, J. Schmidt, and G. M. Schütz, *Proc. Natl. Acad. Sci. USA* **112**, 12645 (2015).
- [11] F. Pollmann, S. Mukerjee, A. G. Green, and J. E. Moore, *Phys. Rev. E* **81**, 020101 (2010).
- [12] C. Karrasch and D. Schuricht, *Phys. Rev. B* **95**, 075143 (2017).
- [13] M. Eckstein, M. Kollar, and P. Werner, *Phys. Rev. Lett.* **103**, 056403 (2009).
- [14] H. U. R. Strand, M. Eckstein, and P. Werner, *Phys. Rev. X* **5**, 011038 (2015).
- [15] H.-J. Lee and R. Bulla, *Eur. Phys. J. B* **56**, 199 (2007).
- [16] R. H. Dicke, *Phys. Rev.* **93**, 99 (1954).
- [17] K. Baumann, C. Guerlin, F. Brennecke, and T. Esslinger, *Nature (London)* **464**, 1301 (2010).
- [18] H.-J. Lee, K. Byczuk, and R. Bulla, *Phys. Rev. B* **82**, 054516 (2010).
- [19] J. Warnes and E. Miranda, *Eur. Phys. J. B* **85**, 341 (2012).
- [20] D. V. Chichinadze, P. Ribeiro, Y. E. Shchadilova, and A. N. Rubtsov, *Phys. Rev. B* **94**, 054301 (2016).
- [21] S. H. Strogatz, *Nonlinear Dynamics and Chaos: With Applications to Physics, Biology, Chemistry, and Engineering* (Westview Press, Boulder, 2014).
- [22] M. J. Feigenbaum, *J. Stat. Phys.* **21**, 669 (1979).
- [23] N. F. Mott, *Metal-Insulator Transitions* (Taylor & Francis, London, 1990).
- [24] T. Furukawa, K. Miyagawa, H. Taniguchi, R. Kato, and K. Kanoda, *Nat. Phys.* **11**, 221 (2015).
- [25] S. V. Streltsov, A. I. Poteryaev, and A. N. Rubtsov, *J. Phys.: Condens. Matter* **27**, 165601 (2015).
- [26] S. Levy, E. Lahoud, I. Shomroni, and J. Steinhauer, *Nature (London)* **449**, 579 (2007).
- [27] P. J. Flory, *Statistical Mechanics of Chain Molecules* (Wiley, New York, 1969).